

Mass Composition and More: Results from the Auger Engineering Radio Array

Bjarni Pont^{a,*} for the Pierre Auger Collaboration^{b,†}

^a*Department of Astrophysics/IMAPP, Radboud University, P.O. Box 9010, NL-6500 GL Nijmegen, The Netherlands*

^b*Observatorio Pierre Auger, Av. San Martín Norte 304, 5613 Malargüe, Argentina*

E-mail: spokespersons@auger.org

The Auger Engineering Radio Array (AERA), as part of the Pierre Auger Observatory, is an array of 153 radio antennas spanning an area of 17 km², currently the largest of its kind, that probes the nature of ultra-high-energy cosmic rays at energies around the transition from Galactic to extra-galactic origin. It measures the MHz radio emission of extensive air showers produced by cosmic rays hitting our atmosphere. We show the recent work by AERA, such as the measurement of the muon content of inclined air showers and the stability of the measured radio signal over almost a decade, as measured with the Galactic radio background. In particular, we highlight the measurements of the depths of the shower maxima X_{\max} , which we use to make inferences about the mass composition of cosmic rays. We reconstruct X_{\max} by comparing the measured radio footprint on the ground to an ensemble of footprints from Monte-Carlo CORSIKA/CoREAS air shower simulations. We compare our X_{\max} reconstruction with fluorescence X_{\max} measurements on a per-event basis, a setup unique to the Pierre Auger Observatory, and show the methods to be fully compatible. We determine the resolution of our method as a function of energy and reach a precision better than 15 g cm⁻² at the highest energies. With a bias-free set of around 600 showers, we find agreement with the Auger fluorescence measurements at energies between 10^{17.5} to 10^{18.8} eV.

*The 27th European Cosmic Ray Symposium - ECRS2022
25-29 July 2022
Nijmegen, the Netherlands*

*Speaker

†Full author list at https://www.auger.org/archive/authors_2022_07.html

1. Introduction

The detection of ultra-high-energy cosmic rays (UHECRs) is only feasible by observation of air showers. Measurements with radio antennas provide sensitivity to the electromagnetic part of the shower. In this proceeding, we present the recent progress of the radio technique at the Pierre Auger Observatory. We present the results from an absolute calibration using the radio emission from the Galaxy in the period of 2014 to 2020. The calibration shows the radio signal to not significantly evolve over the time scale of a decade, providing a new way to investigate the ageing effects of other detection systems such as water-Cherenkov, scintillator, and fluorescence detectors. Furthermore, we show the work on determining the mass composition of cosmic rays. The mass can be inferred from the air-shower observables such as the number of muons and the depth of the shower maximum. The former is used for inclined air showers, i.e., showers with zenith angles above 60° , where water-Cherenkov detectors (WCD) measure a nearly pure muonic signal because the electromagnetic and hadronic shower has been absorbed in the atmosphere before reaching the ground. The combined estimation of this muon signal and the estimation of the shower energy from the radio emission provides sensitivity to the mass of the primary cosmic rays. The second method to probe the cosmic ray mass is used for showers below 55° where the depth of shower maximum, X_{\max} , is used as a mass-sensitive probe.

2. AERA and the WCDs of the Pierre Auger Observatory

The Pierre Auger Observatory [1] is an array of 3000 km^2 , located in Argentina. It measures UHECRs up to the highest energies using 1660 water-Cherenkov detectors (called the surface detector, SD) surrounded by 27 fluorescence telescopes (called the fluorescence detector, FD). The observatory also has an array of radio antennas. The Auger Engineering Radio Array (AERA) [2] covers an area of 17 km^2 and measures the radio signal of air showers at frequencies between 30 and 80 MHz. The array consists of about 150 stations, each with two dipole antennas. This allows for the reconstruction of the electric field at ground level for air showers with energies from 10^{17} (noise-limited) and 10^{19} eV (exposure-limited). The antennas are placed at various spacings (250 to 750 m), allowing for multiple science cases. The denser spacing is more effective for vertically inclined showers where the radio footprints are smaller, while the sparser part, covering a larger area, provides exposure to the larger radio footprints from inclined showers.

3. Absolute calibration and investigation of ageing of the AERA radio signal

A crucial part of precision measurements is the calibration of the equipment. In the past, the calibration of radio antennas was done by characterizing each component in the lab, combining the responses of the whole electronics chain into a total response. Limitations to this approach are present in treating interactions of components and changes over time. Another approach is to evaluate the full signal chain with a known external calibration source (based on [3]). Here, we use the radio background emission from the galaxy.

For this calibration, we analyse the periodically monitored radio signal in each station (every 100 s) for the period of nearly a decade (2014 to 2020). First, we clean the data by removing

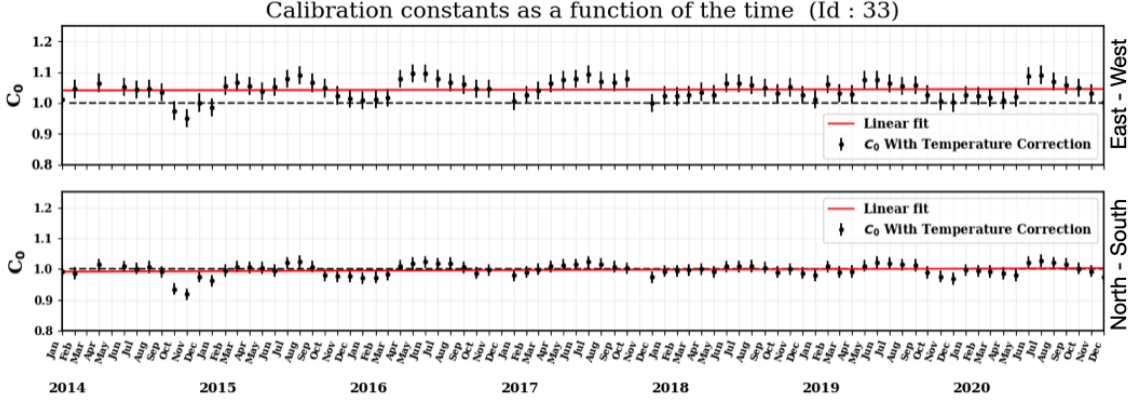


Figure 1: Evolution of the radio signal, expressed as the monthly average of the calibration constants C_0 (black markers) from comparing the measured and modelled galactic radio emission, which acts as a calibration source. Results are shown for both antenna arms (EW and NS) of a single radio station. A linear fit (red line) is shown to investigate the ageing effects of the radio signal.

narrow-band radio frequency interference (RFI) and then we compare the measured power to the expected power from the galaxy. The LFmap software [4] provides a model of the sky based on multiple radio sky surveys.

The expected power P_{sky} and the measured power P_{model} are compared, accounting for the gains of the antenna G_{ant} and electronics G_{RCU} . The comparison also includes a noise term N_{tot} that accounts for ambient broadband RFI and thermal noise from the electronics:

$$P_{\text{model}}(t, \nu) = P_{\text{sky}}(t, \nu) \cdot G_{\text{ant}}(\nu) \cdot G_{\text{RCU}}(\nu) \cdot C_0^2(\nu) + N_{\text{tot}}(\nu), \quad (1)$$

where C_0 is then our frequency-dependent calibration constant, calculated for each antenna arm of each radio station. More details on the method are available in [5].

Fig. 1 shows the calibration constants averaged for each month between 2014 and 2020 for a single station (for both North-South (NS) and East-West (EW) aligned antenna arms). The residual variation is likely due to some residual seasonal temperature effects that remain after having applied a temperature correction. The overall trend is investigated with a linear fit to the monthly averages. We obtain the average slope over all investigated antennas, 1.17 ± 0.29 %/decade (EW) and -0.08 ± 0.26 %/decade (EW), demonstrating no significant trend within uncertainties and at most roughly a 1% effect over a decade of measurements.

These results show that the radio signal is very stable, i.e., shows no significant ageing effects such as do exist for e.g., photo-multiplier tubes (PMTs) in water-Cherenkov detectors or dust accumulation in optical systems such as fluorescence and Cherenkov telescopes. Radio detectors can thus be used to determine an absolute energy scale [6, 7] without additional uncertainty from ageing corrections. Furthermore, it can be used to monitor ageing effects over long periods of time for other types of detectors to reduce uncertainties on air-shower measurements.

4. Measurements of the muon content for inclined air showers

The potential of combined radio emission and muon measurements was shown previously in simulations [8]. In this work, we use air showers measured by both AERA and the WCDs to

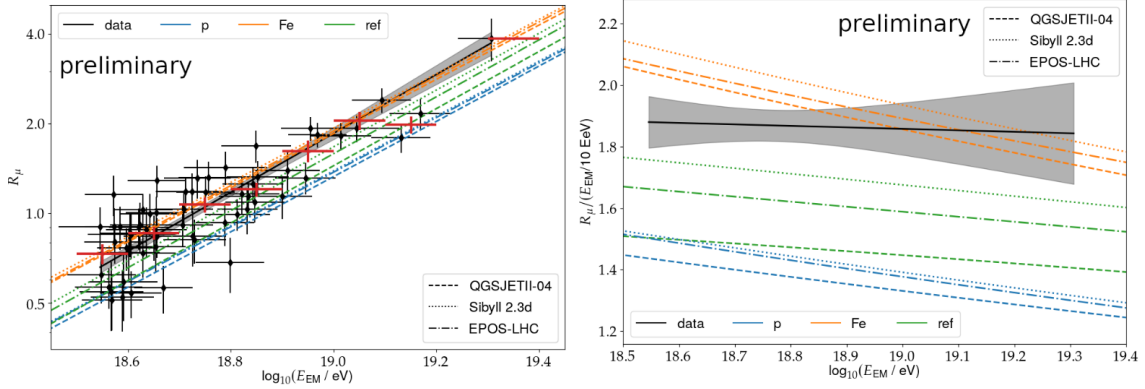


Figure 2: (Left) muon number relative to the muon content of a proton shower at 10^{19} eV simulated with QGSJet II-03 (R_μ) versus the electromagnetic energy (E_{EM}) for measurements (black) and simulations of various compositions, each with three hadronic interaction models. (Right) muon content normalized to the electromagnetic energy to better visualize the comparison to simulations.

measure the muon content of inclined air showers as a function of energy. The number of muons is measured with the WCD and the electromagnetic energy by AERA. We consider zenith angles above 60° such that the WCD measure an essentially pure muon signal since all other particles have been absorbed before reaching the ground. We obtain 59 high-quality events at energies between 4 and 20 EeV. The size of this set is mainly determined by the relatively small AERA surface area (exacerbated by observing at inclined angles, decreasing the effective surface area further) and the current 4 EeV threshold for the WCD.

The measured signals of the WCD are used to scale two-dimensional muon maps in order to derive the muon content. In Fig. 2 (left) we show the relative muon number R_μ , obtained from the scaling of the muon maps w.r.t. a proton-induced shower of 10^{19} eV simulated with the QGSjetII-03 hadronic interaction model. This is plotted versus the electromagnetic energy E_{EM} , determined from fitting a lateral density function (LDF) [9] to the radio emission. The integral of the LDF provides an estimate of the electromagnetic energy in the shower. A linear fit to the data is shown (black line with 1σ confidence band):

$$R_\mu = a \cdot (E_{EM}/10 \text{ EeV})^b. \quad (2)$$

The obtained fit parameters are $a = 1.86 \pm 0.09$ and $b = 0.99 \pm 0.07$. Also shown are the expectations from simulations for a pure proton composition (blue lines for three hadronic interaction models), pure iron composition (orange), and the muon content according to simulations for the composition as measured by the fluorescence detector (FD) of the Pierre Auger Observatory [10]. Fig. 2 (right) shows the muon number scaled by energy to highlight the comparison. The data shows a higher muon content than seen in simulations for the mass composition at Auger. This is commonly known as the muon problem and has been observed by various other studies, e.g., the combined fluorescence light and particle detection at Auger. The new results of the radio-particle technique (when converting E_{EM} to the energy of the primary cosmic ray E_{CR} [6, 7]) provide an estimation of the muon number ($a_{CR} = 1.63 \pm 0.10$ and identical b as before) compatible with the

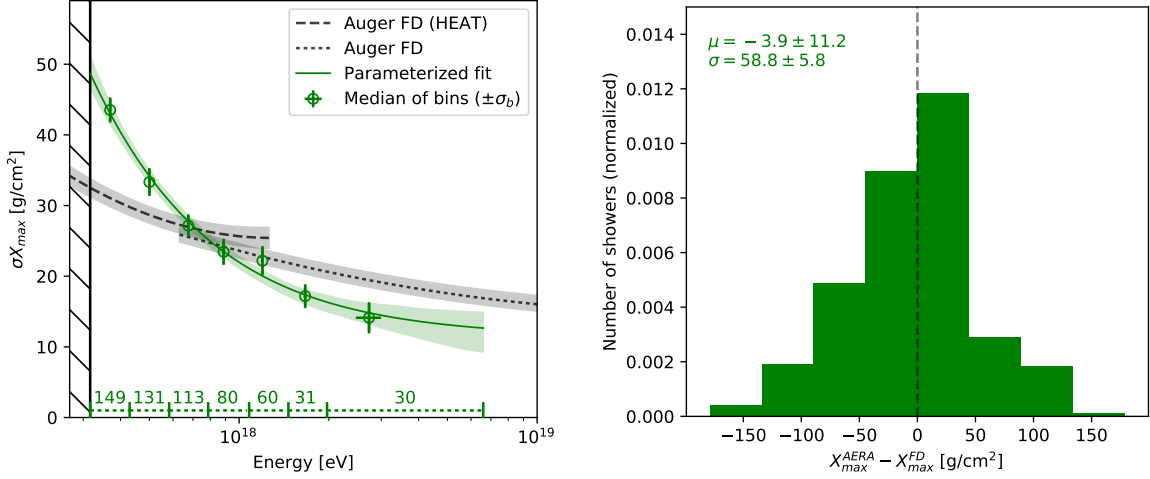


Figure 3: (Left) Median resolution of X_{\max} for our method in several bins in energy (green points) and with a parametrized fit (green line). For comparison, we show the resolution of the Auger FD [15]. Inset at the bottom are the bin size and number of showers per bin. The hatched region on the left indicates a cut at low energy. (Right) Difference of X_{\max} reconstructed with the FD and AERA for a set of showers measured simultaneously with both detectors. Inset at the top are the mean and width of the differences.

fluorescence-particle technique within uncertainties ($a_{\text{CR}} = 1.841 \pm 0.029(\text{stat.}) \pm 0.324(\text{syst.})$ and $b = 1.029 \pm 0.024(\text{stat.}) \pm 0.030(\text{syst.})$). Further details on the method are described in [5].

These new observations are especially relevant considering the upcoming deployment of radio antennas on each of the WCDs, extending our observations from the relatively small AERA surface area to the full 3000 km^2 array [11] allowing us to probe the very highest energies.

5. Measurements of the depth of shower maximum for vertical air showers

For more vertical showers (i.e., below 55°) the radio signal is sensitive to the mass of the cosmic ray primaries by means of how deep in the atmosphere the extensive air shower reaches its maximum (X_{\max}). Generally, protons will interact lower in the atmosphere than heavier particles like iron nuclei and as such we can determine the mass composition by comparing measurements of many showers to air shower simulations.

We use the observation of over 2000 showers with AERA and the WCDs and for each we simulate air showers using CORSIKA/CoREAS [12, 13] in order to reconstruct X_{\max} by comparing their radio signals. Details on the method are described in [14]. After quality cuts and fiducial cuts we obtain a set of 594 air showers with high quality X_{\max} estimation and free of selection effects at energies between $10^{17.5}$ to $10^{18.8}$ eV. In Fig. 3 (left) we show the median resolution we obtain with our method as a function of the shower energy (green) showing the method to be competitive with the fluorescence method to measure X_{\max} [15]. The resolution for AERA increases with energy as the radio footprint on the ground increases in both amplitude and size (i.e., good SNR in more stations). In addition, for a set of 53 showers we also have an independent reconstruction of X_{\max} by the fluorescence detector allowing us to compare our method to the fluorescence method on an event-to-event basis. Fig. 3 (right) shows the difference in X_{\max} for this hybrid data set, demonstrating good agreement and no significant bias within statistical uncertainties

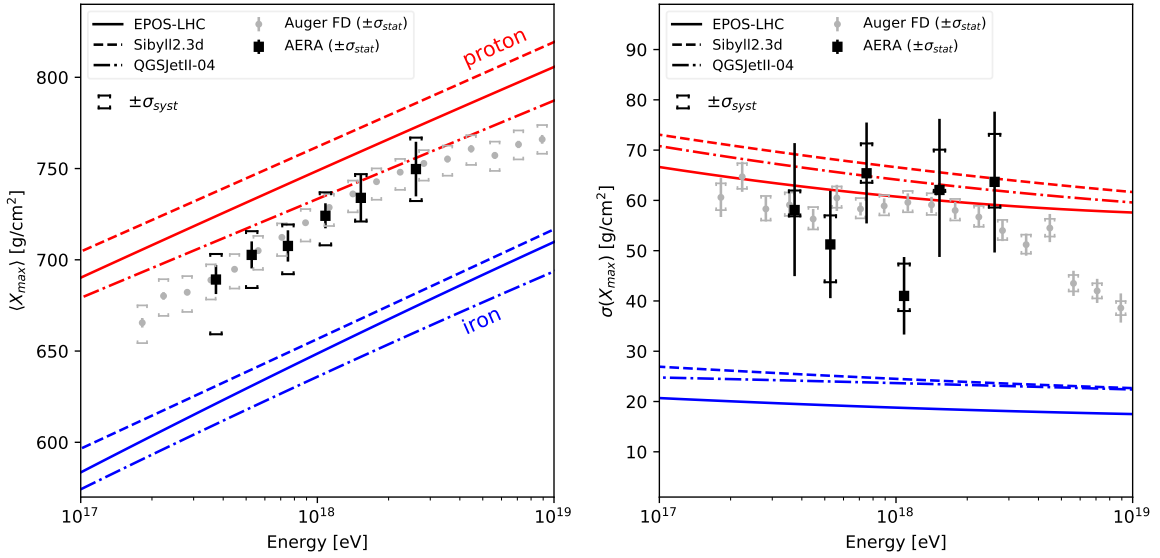


Figure 4: Weighted mean (left) and width (right) of the X_{\max} distribution in six energy bins as measured by AERA (black). Shown for comparison are the X_{\max} moments of the Auger FD [10] and the predictions of air shower simulations for a composition of only protons (red) and only iron nuclei (blue) for three hadronic interaction models. Systematic uncertainties are indicated with capped markers and statistical uncertainties with vertical bars.

($X_{\max}^{\text{AERA}} - X_{\max}^{\text{FD}} = -3.9 \pm 11.2 \text{ g cm}^{-2}$). The spread of the difference is compatible with the combined resolution of the FD and our method, indicating further agreement.

To interpret the X_{\max} values of the 594 air showers in terms of the primary masses of the cosmic rays we show the first two moments of the X_{\max} distribution as a function of energy in Fig. 4. We demonstrate good agreement with the Auger FD measurements over our entire energy range, further supporting the results of the 53-event hybrid set of events. For comparison, we show the first moment as predicted by three hadronic interaction models for a mass composition consisting of only protons (red) and only iron nuclei (blue). The right figure shows the second moment of X_{\max} and similarly, it shows compatibility with the FD results.

With these results, we demonstrate that the radio technique is able to reconstruct X_{\max} with high resolution. Furthermore, by measuring X_{\max} with multiple techniques at the Pierre Auger Observatory we have been able to show the two methods are in agreement and as such the radio technique is shown to be viable as a technique that can operate as cross-check for other techniques or as a (lower-cost) alternative.

6. Conclusion

In this work, we have shown the recent progress at AERA. By performing measurements of the Galactic background sky we have implemented an absolute calibration and validated the lab measurements of the the signal response. With this, we have demonstrated this calibration, and thus the radio signal, to be stable over almost a decade of measurements, providing a new way to cross-calibrate other detector systems that do suffer from ‘ageing’ of their systems. We have also presented two methods to investigate the mass composition of cosmic rays. For inclined events

we have used the muon measurements of the WCD and electromagnetic energy measurements of AERA to demonstrate an independent way to measure the muon content in air showers (in agreement with WCD-FD measurements), laying the foundation for the 3000 km² radio array currently being deployed. For vertical showers we have shown the results of measurements of the mass-sensitive probe X_{\max} and have demonstrated we are able to achieve a resolution competitive with the FD. We obtained results that are in agreement with the FD, both for X_{\max} measurements for a subset of simultaneously measured air showers and for the first two moments of the X_{\max} distribution, demonstrating the strength and feasibility of the radio technique to do mass-sensitive measurements.

References

- [1] A. Aab *et al.* (Pierre Auger Collaboration), *Nucl. Instrum. Meth. A* **798** (2015) 172–213
- [2] P. Abreu *et al.* (Pierre Auger Collaboration), *J. Instrum.* **7**, P10011 (2012).
- [3] K. Mulrey, *Astropart. Phys.* **111**, 1-11 (2019).
- [4] E. Polisensky, *Long Wavelength Array Memo Series* **111**, 1 (2019).
- [5] R. M. de Almeida *et al.* in *Proceedings of the 9th International Workshop on Acoustic and Radio EeV Neutrino Detection Activities*, **PoS(ARENA2022)039** (2023).
- [6] A. Aab *et al.*, *Phys. Rev. Lett.* **116**, 241101 (2016).
- [7] A. Aab *et al.*, *Phys. Rev. D* **93**, 122005 (2016).
- [8] E. M. Holt, F. G. Schröder, and A. Haungs, *Eur. Phys. J. C* **79**, 371 (2019).
- [9] F. Schlüter, Felix and T. Huege, *JCAP* **01**, 008 (2023).
- [10] A. Yushkov [for the Pierre Auger Collaboration], **PoS(ICRC2019)482**
- [11] F. Schlüter [for the Pierre Auger Collaboration], **PoS(ICRC2021)262**
- [12] D. Heck *et al.*, *FZKA Tech. Umw. Wis. B* **6019** (1998)
- [13] T. Huege *et al.*, *AIP Conf. Proc.* **1535** (2013) 128-132
- [14] B. Pont [for the Pierre Auger Collaboration], **PoS(ICRC2021)387**
- [15] J. Bellido [for the Pierre Auger Collaboration], **PoS(ICRC2017)506**